Dergi Listesi

Dergi Adı

ISSN 1369-8001

Yıl 2021

Temizle Ara

No	Yıl	Dergi Adı	ISSN	Çeyreklik Grup	Katsayı	kategori	Dergi Puanı
99608	2021	MATERIALS SCIENCE IN SEMICONDUCTOR PROCESSING	1369-8001	Q1	1	SCIE	

Sayfada 10 Kayıt Göster

Önceki 1 Sonraki

1 Kayıttan 1 - 1 Arası Kayıtlar

Materials Science in Semiconductor Processing 142 (2022) 106464

Contents lists available at ScienceDirect

Materials Science in Semiconductor Processing

journal homepage: www.elsevier.com/locate/mssp

Growth and characterization of PALE Si-doped AlN on sapphire substrate by MOVPE

Kağan Murat Pürlü [a], Merve Nur Koçak [a,b], Gamze Yolcu [a,b], İzel Perkitel [a,c], İsmail Altuntaş [a,c], Ilkay Demir [a,c,*]

[a] Nanophotonics Research and Application Center, Sivas Cumhuriyet University, 58140, Sivas, Turkey
[b] Department of Metallurgy and Materials Engineering, Institute of Science, Sivas Cumhuriyet University, 58140, Sivas, Turkey
[c] Department of Nanotechology Engineering, Faculty of Engineering, Sivas Cumhuriyet University, 58140, Sivas, Turkey

ARTICLE INFO

Keywords:
AlN
MOVPE
Si doped
Pulsed atomic layer epitaxy

ABSTRACT

In this study, we report different SiH_4 flow condition effects on crystal, surface, optical, and electrical characteristics of heteroepitaxial Metal-Organic Vapor Phase Epitaxy (MOVPE) grown AlN layers on sapphire substrates. Adjustment of growth kinetics is very important to control the doping. Therefore, pulsed atomic layer epitaxy (PALE) was used to control the growth kinetics and reduce parasitic reactions that inevitably caused adverse impact on the properties of the epitaxial AlN films. As a result of HRXRD (high resolution x-ray diffraction) analysis, the (002) ω FWHM decreased significantly with the PALE method, while the increase occurred due to the development of V defects for the (102) ω scan. Atomic force microscopy (AFM) analyzes showed that SiH_4 led to a 3D-like growth mode. It was demonstrated that the increased SiH_4 flow increased Si incorporation into the Si-doped AlN layer while increased the sheet resistance due to the self-compensating effect obtained from secondary ion mass spectroscopy (SIMS) and I–V measurement results.

1. Introduction

AlN has possessed huge potential in power electronics and deep UV (ultraviolet) optoelectronics since it has important properties such as a large bandgap energy of 6.2 eV and a critical electric field of up to 12 MV/cm [1,2]. The performance or efficiency of these device applications depends on the quality of the used AlN epitaxial film. It is necessary to use one of the growth techniques which are either AlN on AlN substrate (homoepitaxy) or AlN on foreign substrate (heteroepitaxy) to obtain a high quality AlN epitaxial films. Although the best option for the development of high performance devices is the homoepitaxial growth of AlN films, this is not preferred owing to its limited size and high cost. It is very difficult to obtain high-quality AlN films with less stress and highly controllable impurity level at high temperatures even though foreign substrates has advantages such as lower cost and larger size [3]. Sapphire, one of the foreign substrates, is the most favorable substrate because of its high-temperature stability as well as its low cost and wide availability. Threading dislocations are inevitably occurred due to a large lattice mismatch and thermal expansion coefficient difference between AlN and sapphire substrate, resulting in adverse impact on the properties of the epitaxial thin film. Many approaches such as using the buffer layer, ELOG, PALE growth, etc. have been used to overcome the formation of the dislocations [4]. The intentional doping of the AlN layer, which is also the focus of this study, is important both to reach the desired electrical conductivity and to control the carrier concentration [5]. However, very limited reports due to obstacles faced in the heteroepitaxial growth of high-quality AlN layers have been so far published about the transport phenomenon and properties of intentionally doped AlN in the literature [6,7]. It is predicted that Si, which is generally used for intentional n-type doping of AlN [8] readily induces the formation of defect complexes resulting in suppressing the motions of charge carriers. Although such defect complexes are simulated by control of chemical potential and Fermi level [6,7], the comprehending impact of line defects such as threading defects on doping distribution and defect complexes is important for full control of the development of the desired device. Adjusting the growth kinetics is very important in the control of doping [9,10] and this can be supported by previously published studies about AlN-related alloys grown via the MOCVD system [9–11]. It is known that chemical, electrical and structural properties of any material system can be affected by reactions between precursors which are placed

* Corresponding author. Nanophotonics Research and Application Center, Sivas Cumhuriyet University, 58140, Sivas, Turkey.
E-mail address: idemir@cumhuriyet.edu.tr (I. Demir).

https://doi.org/10.1016/j.mssp.2022.106464
Received 6 July 2021; Received in revised form 3 January 2022; Accepted 5 January 2022
Available online 10 January 2022

in the gas-phase and near the hot deposition surface [12]. Many groups continue still to carry out studies about the behavior of doping and how the level of doping concentrations can be increased since the proper doping of AlN layers to obtain reasonable electrical conduction for device applications is a key issue. Some of these studies are as follows: Thapha et al. have done studies about optimization of the growth process to obtain a high-quality n-AlN layer by using MOCVD [13]. Their finding results show that both crystal quality and surface morphology start to deteriorate due to in-plane tensile strain at a higher Si concentration (2×10^{19} cm^{-3}) [13]. M. Hermann et al. have investigated the influence of the growth conditions on the Si incorporation into AlN films grown by plasma-assisted molecular-beam epitaxy [14]. They have reported that although Al-rich growth condition is suppressed Si incorporation, nitrogen-rich growth condition allows controlled incorporation of Si up to a concentration of 5.23×10^{21} cm^{-3} [14]. M. Hayden Breckenridge et al. have shown the influence of how Si implantation parameters and activation annealing processes on the structural and electrical properties of AlN films [15]. They have obtained the Si implanted AlN sample which is a uniform doping profile with a peak depth of ~120 nm, peak Si concentration of 9×10^{18} cm^{-3}, and low activation energy of ~70 meV [15].

In this study, we investigated the effect of the growth conditions having different flow rates and times on crystal, optical, and electrical properties of n-type AlN grown on sapphire substrate by MOVPE. The pulsed flows, known as PALE growth, and the continuous flows have been supplied during the growth of Si-doped AlN. While TMAl and NH_3 sources during Si-doped AlN growth have been supplied to the reactor as a pulse, SiH_4 gas has been provided as continuous, together with TMAl as pulse, together with NH_3 as pulse, and pulse between the flows TMAl and NH_3. The schematic representation of the above-mentioned flow diagram is given in the experimental section. The obtained results show that the quality of the Si-doped AlN layer, both in terms of crystal and electrical, is better when SiH_4 gas is supplied to the reactor as a pulse compared to the case where it is provided as a continuous. The characterization systems such as high-resolution X-ray diffractometer (HR-XRD), atomic force microscopy (AFM), UV-VIS-NIR spectrophotometer, raman spectroscopy, current-voltage, and secondary ion mass spectroscopy (SIMS) have been utilized to analyze Si-doped AlN layer grown on sapphire by MOVPE.

2. Experimental

Si-doped AlN epilayers were grown on 2" diameter c-plane sapphire substrates by MOVPE system. Al and N atoms are obtained from trimethylaluminum (TMAl) and ammonia (NH_3) precursors, respectively. H_2 and N_2 are used as carrier gas. At first, thermal desorption of the sapphire substrate was carried out at 1400 °C for 10 min under H_2 ambient to remove the purities such as surface contamination and adsorbed water. After that, a ~30 nm thick AlN nucleation layer (NL) having TMAl flow of 5.17×10^{-6} mol/min and NH_3 flow of 1200 sccm was grown at 1075 °C and 50 mbar reactor pressure. Subsequently, high-temperature AlN was grown on the AlN nucleation layer. It is known that strong parasitic gas-phase reactions between TMAl and NH_3 during AlN growth decrease the growth rate and negatively affect the surface morphology of the thin film [15,16]. The PALE technique in which TMAl and NH_3 precursors are supplied to the reactor separately has been widely used to minimize the effect of the parasitic reactions. The growth mechanism of the PALE AlN can be found in our previous study [17]. The high-temperature AlN layer is divided into two parts as u-AlN (undoped AlN) and Si-doped AlN. Firstly, unintentionally doped AlN with 300 loops was grown at 1440 °C and 50 mbar by using the PALE technique with optimized alternating 4s pulse of TMAl and 2s pulse of NH_3 sources [17]. Secondly, Si-doped AlN with 300 loops was grown under three different conditions: the continuous flow of SiH_4, pulse SiH_4 source with TMAl or NH_3, and pulse SiH_4 source between TMAl and NH_3. The main purpose in these three different cases is to obtain AlN layers with high crystal quality, high carrier density, and smooth surface. In the first condition, SiH_4 flow was supplied continuously during Si-doped AlN growth. And, SiH_4 flow rates were changed as 2.23×10^{-6}, 8.92×10^{-6}, and 17.8×10^{-6} mol/min to investigate the influence on properties of the AlN layer. In the second condition, pulse SiH_4 source together with TMAl or NH_3 has been supplied to the reactor. The results obtained from these growths are important to find the relationship of SiH_4 source with the used TMAl and NH_3 sources. In the third condition, pulse SiH_4 flow was supplied between TMAl and NH_3 precursors. Pulse SiH_4 flow time was changed as 1, 3, and 5 s. Whole growths made in this context were carried out at 1440°C reactor temperature and 50 mbar reactor pressure. The TMAl and NH_3 flow rates used in PALE AlN growth are the same as those used in the nucleation layer. These HT-AlN samples were named as A for continuous SiH_4 flow, B (C) for SiH_4 flow together with TMAl (NH_3), and D for pulse SiH_4 flow between TMAl and NH_3 and are briefly summarized in Table 1.

The schematic view of the growth structure (Fig. 1-a) consists of the AlN buffer layer, resistive u-AlN layer, Si-doped AlN layer, and contact metals. The on-off time sequences of sources (SiH_4, NH_3, and TMAl) used during PALE Si-doped AlN growths are given in Fig. 1 b-e for different SiH_4 flow conditions.

HR-XRD and AFM were utilized to investigate the effect of different SiH_4 conditions used during Si-doped AlN growth on crystalline and surface quality for all samples, respectively. Optical transmission spectra were characterized using spectrophotometer. The silicon (Si) concentrations of grown PALE-AlN epilayers were investigated by secondary ion mass spectroscopy (SIMS). After the characterization measurements were done, the samples were cut 1×1 cm^2 for the electrical measurements, and then followed by chemical cleaning. Afterward, the samples were deposited with Ti/Al/Ti/Au (20/100/20/50 nm) and Ni/Au (20/50 nm) for Ohmic and Schottky contacts, respectively. Ohmic contacts were annealed at 1025 °C for 35 s in N_2 environment. Electrical properties of Si-doped AlN with Ohmic and Schottky contacts are investigated by Keithley IV-CV measurement system.

3. Result and discussions

Variation of 2x2 μm^2 AFM surface morphologies of Si doped AlN samples grown under three different SiH_4 flow conditions are given in Fig. 2. The effect of continuous SiH_4 flows (A1, A2, and A3) on the crystalline quality and surface morphology are studied by measuring (002) symmetric diffraction-(102) symmetric diffraction in skew geometry ω scans and rms roughnesses by HRXRD and AFM, respectively. Fig. 4 a) shows the FWHM values of (002) and (102) rocking curves of the AlN samples grown with continuous SiH_4 flow. The results obtained from the HRXRD measurements show that there is not much significant effect of SiH_4 flow on crystalline quality of Si-doped AlN samples. It is seen that the (002) rocking curve FWHM almost does not change while the (102) one tends to decrease with increasing SiH_4 flow. FWHM values are widely used to obtain dislocations in AlN epitaxial films [18]. The screw and edge type dislocations are associated with the FWHM values obtained from (002) and (102) rocking curve ω scans, respectively. The calculated screw and edge type dislocation density values for all samples are given in Table 2 and Fig. 3. The increase in the SiH_4 flow rate creates a higher tilt and twist in the sub-crystalline grains, resulting in an

Table 1
Si-doped AlN samples with grown under three different SiH_4 flow conditions.

Sample	SiH_4 flow
A	**Continuous**
(A1, A2 and A3)	(2.23 (A1), 8.92 (A2) and 17.8 (A3) μmole/min)
B	**Pulse with TMAl**
C	**Pulse with NH_3**
D	**Pulse between TMAl and NH_3**
(D1, D2, and D3)	(1s (D1), 3s (D2), and 5s (D3))

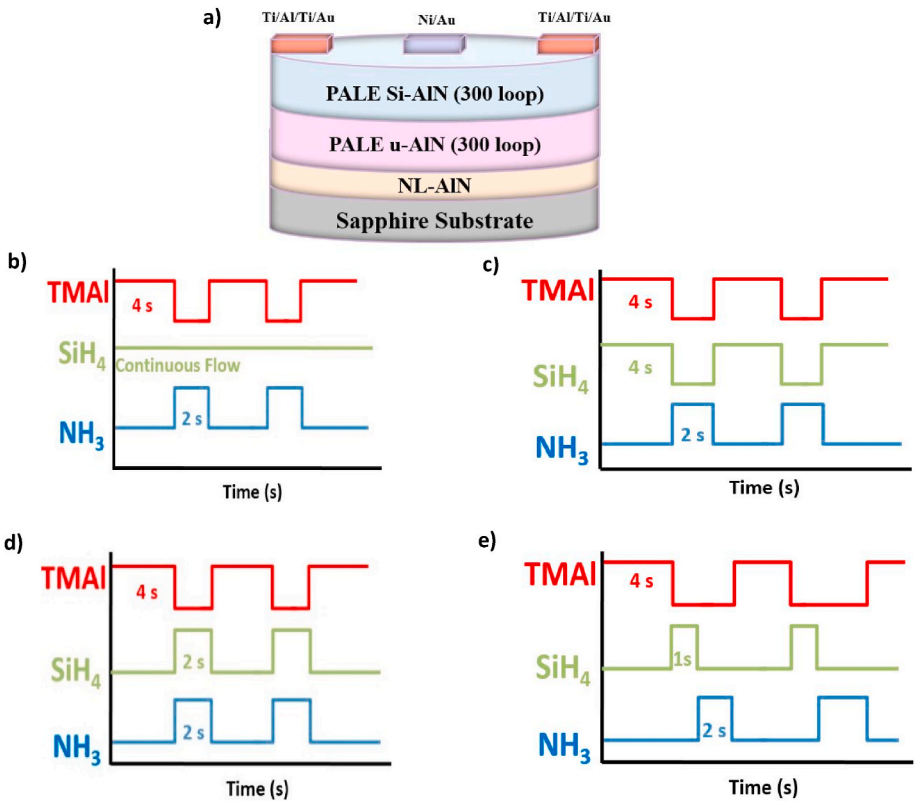

Fig. 1. Schematic view of the growth structure (a), flow diagrams of different SiH_4 flow conditions: continuous SiH_4 flow (b), pulse SiH_4 flow together with TMAl (c) or NH_3 (d), and pulse SiH_4 flow between TMAl and NH_3 (e).

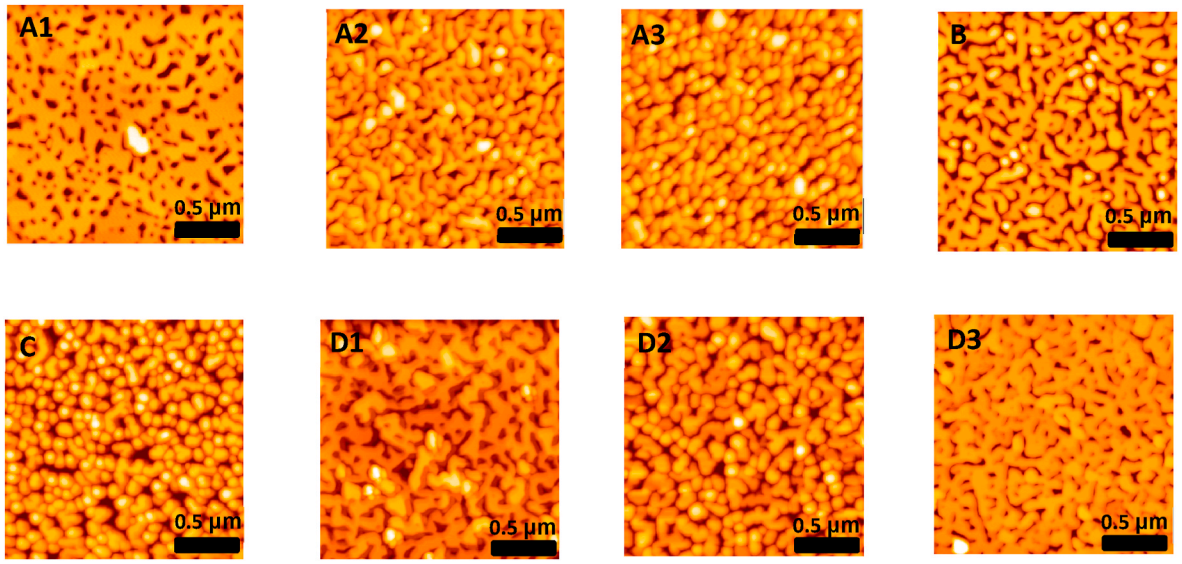

Fig. 2. Variation of 2 × 2 μm^2 AFM surface morphologies of Si doped AlN samples grown under three different SiH_4 flow conditions.

increase in stacking faults [19]. For this reason, as stacking faults and dislocations along the growth planes resulting from the increased tilt between the sub-crystallines interact with the threading dislocations, edge type dislocations in the AlN layer have reduced. On the other hand, the screw-type dislocation is not likely to be eliminated because of the requiring a pair of screw dislocations with opposite Burgers vectors along the growth direction [20].

In terms of the surface morphology, Fig. 4 b) demonstrates that the increasing SiH_4 flow degrades the surface quality by increasing the rms roughness [21]. It has been seen that all Si-doped AlN samples have rough surface morphology formed by hexagonal faceted nano-columns because SiH_4 acts as an anti-surfactant and leads to three-dimensional (3D) growth [22]. This 3D surface growth model supports columnar growth which has a greater growth rate on the vertical side than that of the lateral side. A similar surface shaped has been seen due to the use of the high nitridation time and high V/III ratio [23–25].

In order to understand both the incorporation mechanism and the effect of SiH_4 on the properties such as crystalline quality and surface morphology of AlN epilayer, SiH_4 precursor has been supplied to the reactor with TMAl (sample B) and with NH_3 sources (sample C). Fig. 5

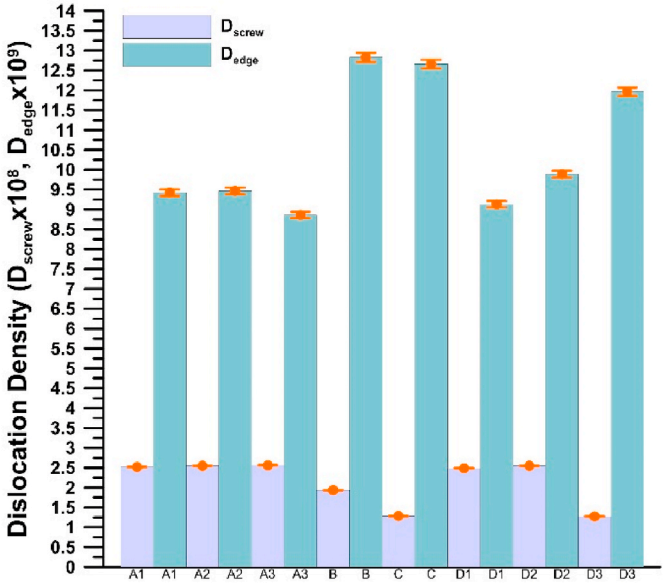

Fig. 3. Screw and edge type dislocation densities for all samples with error bars.

shows the FWHM values of (002) and (102) ω scans of samples which are 298 and 243 arcsec for (002) plane and 1516 and 1506 arcsec for (102) plane, respectively. These values correspond to 1.93×10^8, 1.29×10^8 cm^{-3} screw and 1.28×10^{10}, 1.27×10^{10} cm^{-3} edge dislocation density respectively. There is ~33% improvement in screw dislocation density and ~1% in edge dislocation density by co-pulsed of SiH_4 with TMAl, and NH_3, respectively. While the (002) plane XRD FWHM value do not change with continuous SiH_4 flow it is decreased down to 242 arcsec with the introducing of the PALE SiH_4 which indicates that the PALE technique plays an important role in the control of crystal quality and improved interface between epilayers and substrate [26]. Al adatoms have a low surface diffusion however, residual Si precursors cause further reduction of surface diffusion. During the co-pulsed of SiH_4 and NH_3, PALE technique plays a role in eliminating the edge dislocations since it enhanced the adatom mobility [26–29]. Si precursors acts as an anti-surfactant that causes tensile strain during growth. This leads to a decreased critical layer thickness for such relaxation processes results with cracking, pitting or roughening [5,13,30,31]. However, with the co-pulsed of SiH_4 and NH_3 it is thought that passivation decoration of the TDs by either the Si atoms or Si_xN_y masking followed [21,32]. In-situ SiN_x masks formed by decomposition of SiH_4 and NH_3 are generally used for defect reduction in GaN [33,34]. It has been shown that this application can be beneficial in $Al_xGa_{1-x}N$ compositions with x below 0.4, but there are no reports for Al composition above x = 0.4 [22,35]. To the best of our knowledge, no reports exist on the use of in-situ SiN_x mask for defect reduction in AlN. However, further analysis and simulation of possible Si–Al–N structure componds are required to prove this hypothesis [36].

AFM images of sample B and C are also be inserted in Fig. 5 and it is also seen from the Figure that SiH_4 flow with TMAl results in lower rms roughness value of surface. This led to the thought that the increase in surface roughness after treatment with co-impact SiH_4 and NH_3 might be due to the strain occurred. Surface rms roughness values are 7.98 and 11.68 nm for $5 \times 5\mu m^2$ scan area and both samples have hexagonal nano columns on the surface. It is also observed that the growth rate of B and C samples are not much different depending on whether SiH_4 is supplied with TMAl or NH_3.

As a third technique, three samples have been grown with separate pulse of SiH_4 as shown in Fig. 6. Also the pulse duration of SiH_4 is changed between 1s and 5s. Fig. 6 shows the FWHM values of grown samples. As it can be seen clearly, from the figure that the flow duration of pulsed SiH_4 between TMAl and NH_3 improved the screw dislocation density almost 49% and the surface roughness down to ~1 nm. However, the increasing SiH_4 flow duration slightly increased the edge type dislocation density. However, the increased SiH_4 flow duration caused the development of V defects such as stacking mismatch boundary (SMB) and hexagonal micro-pit (HMP) defects, resulting in a slight

Table 2
The obtained FWHM values of (002) and (102) and corresponding screw and edge type dislocation densities for all samples.

	FWHM ω(002) (arcsec)	D_{screw} (cm^{-3})	FWHM ω(102) (arcsec)	D_{edge} (cm^{-3})
Sample A1	340	$2.52 \times 10^8 \pm 0.004$	1299	$9.42 \times 10^9 \pm 0.083$
Sample A2	342	$2.55 \times 10^8 \pm 0.004$	1302	$9.46 \times 10^9 \pm 0.083$
Sample A3	343	$2.56 \times 10^8 \pm 0.004$	1260	$8.86 \times 10^9 \pm 0.078$
Sample B	298	$1.93 \times 10^8 \pm 0.003$	1516	$1.28 \times 10^{10} \pm 0.113$
Sample C	243	$1.29 \times 10^8 \pm 0.002$	1506	$1.27 \times 10^{10} \pm 0.111$
Sample D1	338	$2.49 \times 10^8 \pm 0.004$	1279	$9.13 \times 10^9 \pm 0.080$
Sample D2	342	$2.55 \times 10^8 \pm 0.004$	1331	$9.89 \times 10^9 \pm 0.087$
Sample D3	242	$1.28 \times 10^8 \pm 0.002$	1464	$1.20 \times 10^{10} \pm 0.105$

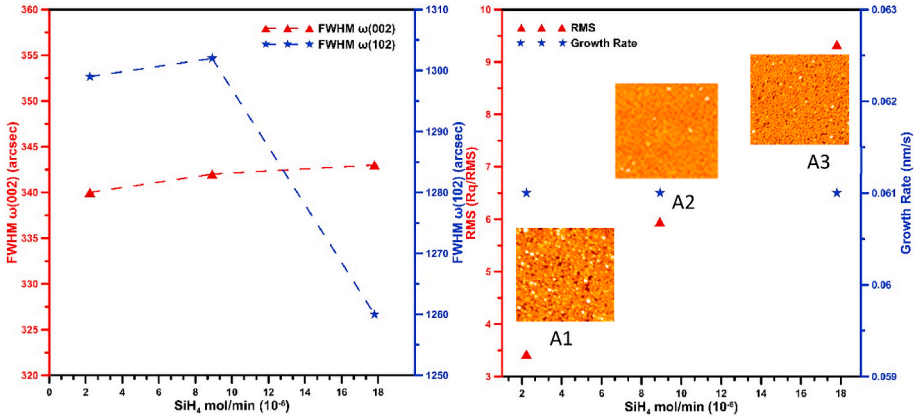

Fig. 4. a) The variation of (002) symmetric diffraction (red) and (102) symmetric diffraction in skew geometry (blue) FWHM (red line) values, b) the variation of 5 × 5 μm^2 AFM surface morphologies and growth rates with the increased SiH_4 flow rates for A1, A2, and A3.

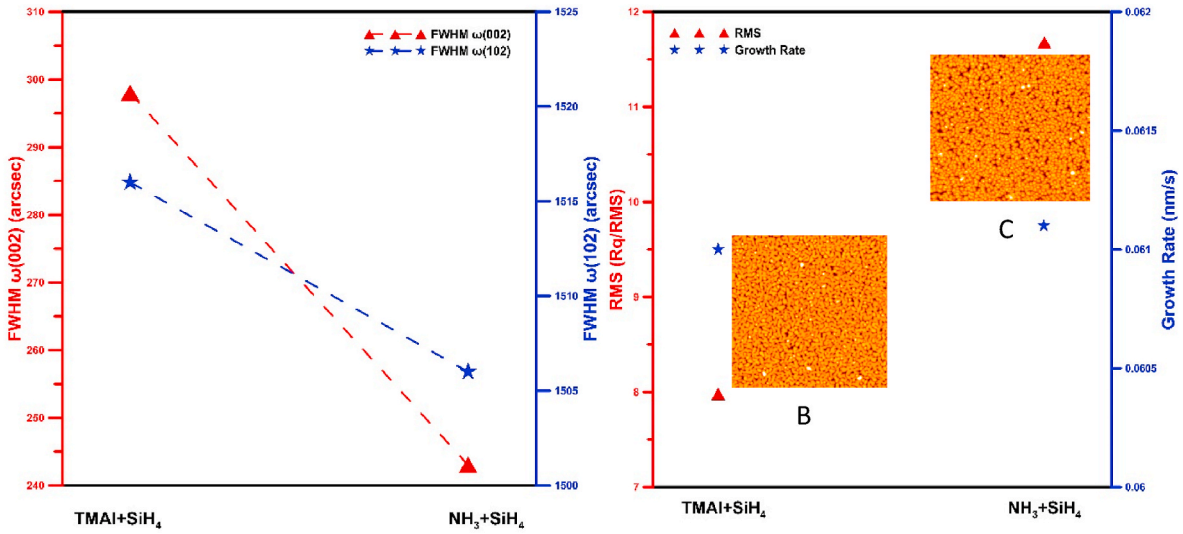

Fig. 5. a) Symmetric diffraction (002) and symmetric diffraction in skew geometry (102) FWHM values when SiH_4 precursor is supplied to the reactor with TMAl (example B) and with (example C) b) 5 × 5 μm^2 AFM surface morphologies and growth rate of B and, C.

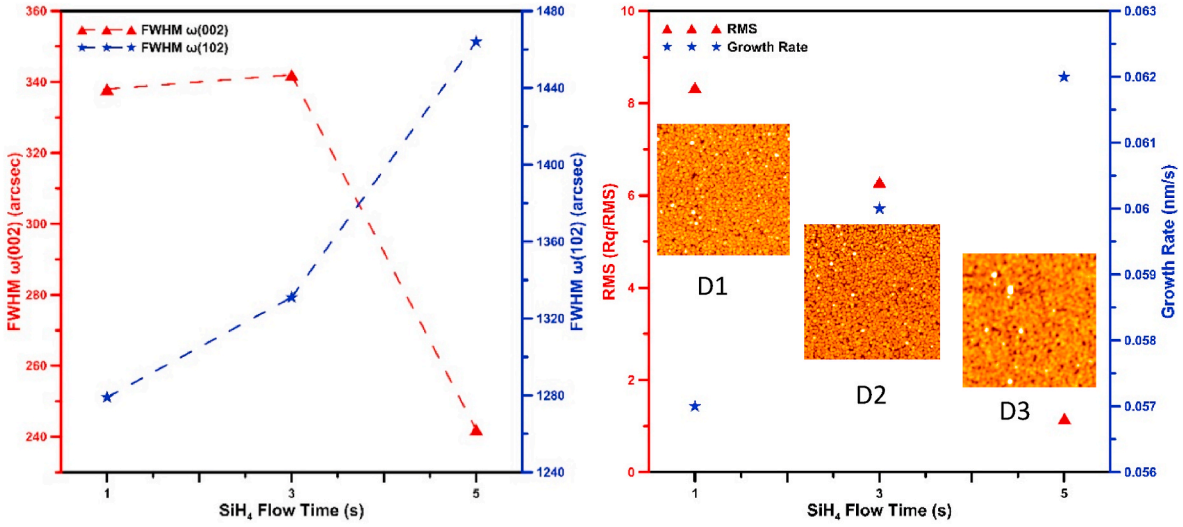

Fig. 6. a) Symmetrical diffraction (002) and symmetric diffraction in skew geometry (102) FWHM values as a result of the variation of pulse SiH4 flow between TMAl, NH_3 between and SiH_4 pulse duration 1s–5 s b) 5 × 5 μm^2 AFM surface morphologies and growth rate of D1, D2 and, D3.

increase in the edge type dislocation density [20]. It can be concluded that the increasing SiH_4 pulse duration increased D_{edge}, since it is believed that increasing time delay between group III precursors gives an appropriate time to bonding with less parasitic reaction.

With three growth techniques (two proposed in this study) continuous, co-pulsed with precursors, pulsed independently obtained results were compared. In continuous flow study reasonable crystalline quality obtained with hexagonal nano columns appear to be dominant in surface images. In the co-pulsed with precursors study, it is observed that the technique played a role in the reduction of dislocations by increasing the mobility of Al adatoms and forming Si_xN_y masking. However, hexagonal nano-columns were still observed in the surface images. With a final technique, separately pulsed of SiH_4, lower dislocation density and surface roughness are obtained.

Fig. 7 shows the transmittance spectra of samples A1, C and D3 in the 200–800 nm range. In the spectral region of high transmittance, discrete interpenetrating circles appear. Samples begin to absorb incoming light where the wavelength is short. The density of the interpenetrating circles decreases and disappears when the absorption edge appears. In

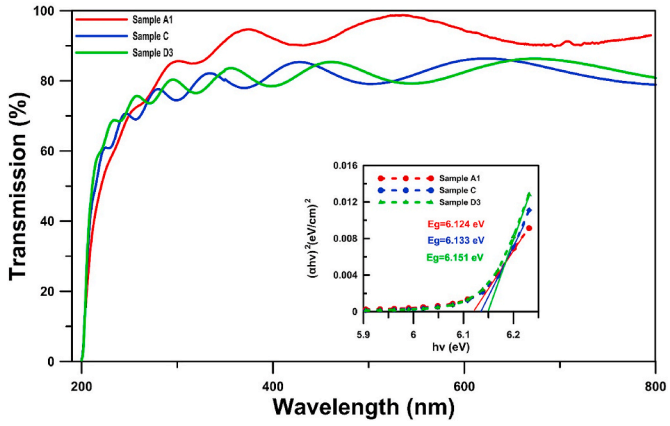

Fig. 7. Sample A1, C and, D3 the transmittance spectra in the wavelength range from 200 to 800 nm, and plot of $(\alpha h\nu)^2$ vs hν determined by transmission measurement.

Fig. 7 the high quality and surface homogeneity of AlN films can be seen from the appearance of the interpenetrating circles by pulsed independently PALE method. As shown in Fig. 7, as the SiH_4 flow continuous, co-pulsed and pulsed independently the optical transmittance shifts towards a higher energy region, respectively. In other words, it can be said that the optical absorption edge is shifted to higher energy. The reason of this behaviours thought that is the improvement of the crystallinity of AlN films. Also in Fig. 7, optical band gap values were estimated by extrapolating the linear part from the graph of photon energy ($h\nu$) versus $(\alpha h\nu)^2$. While the SiH_4 flow was continuous, the energy band gap Eg was 6.124 eV, the increased to 6.133 eV for co-pulsed, and finally the E_g increased to 6.151 eV for pulsed independently. These values are slightly lower than the literature values for bulk AlN and can be attributed to the stress difference along these axes. The increase in absorption band energy is attributed to the increase in film quality as a result of SiH_4 doping with PALE. These results support the HRXRD findings.

The Raman measurements carried out to analyze the strains in A1, C, and D3 epilayers have been shown in Fig. 8. The E2(high) peak frequency at 657 cm^{-1} in the Raman spectra is the natural state used for strain measurement of AlN. The E2(high) peak frequency for Sample A1, C, and D3 in Raman spectra have been seen at 659.0, 655.6, and 656.7 cm^{-1}, respectively (Table 3). It is known that the Raman peak corresponding E2(high) shifts to a higher frequency due to compression stress and to a lower frequency due to tensile stress [37]. In the inset in Fig. 8, the change of the position of E2(high) peak frequency according to the flow state of Silane is given and a slight shift has been observed. Sample A1 indicates the existence of compression stress while Sample C and D3 indicate the existence of tensile strain. Besides, stress and strain in in-plane and out-plane have been calculated for Sample A1, C, and D3 by using the following equations:

$$\sigma = \frac{(\text{phonon peak shift})}{K} \quad (1)$$

$$\varepsilon = \frac{\sigma}{\Upsilon} \quad (2)$$

where K is the pressure coefficient of 4.3 cm^{-1} GPa^{-1}, σ is the in-plane stress and ϒ is the biaxial stress of AlN of 469 GPa [37,38]. The values of in-plane and out-plane stress (strain) have been obtained -0.465 GPA (-0.0991), 0.325 GPA (0.0682), 0.069 GPA (0.0148) for Sample A1, C and, D3 respectively (Table 3).

We have measured with a four-point probe the sheet resistance of grown samples to check the effect of proof of concept growth techniques

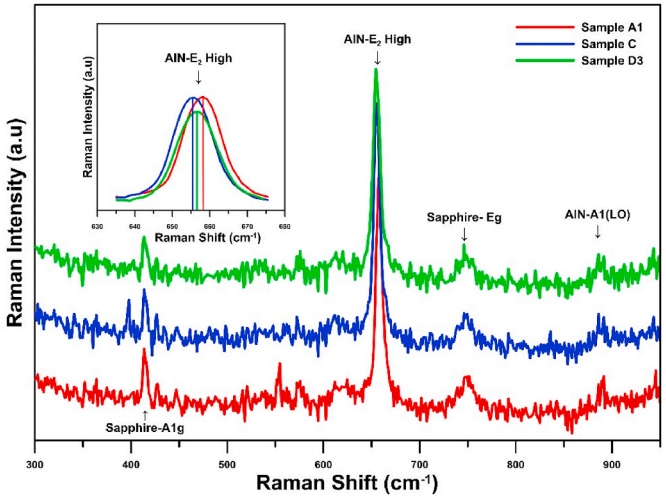

Fig. 8. Raman spectra of AlN grown on sapphire substrate with grown under three different SiH_4 flow conditions. (Continuous flow A1, Pulse with NH_3 C, and Pulse between TMAl and NH_3 D3).

Table 3
Results of the Raman spectra of AlN grown on sapphire substrate.

Sample name	Wavenumber (cm^{-1})	In-plane and out-plane stress (GPa)	In-plane and out-plane strain (%)
A1	659	−0.465	−0.0991
C	655.6	0.325	0.0682
D3	656.7	0.069	0.0148

on electrical properties by I–V measurements shown in Fig. 9 b. It has been observed that there is three magnitude of order improvement of sheet resistance of separately pulsed SiH_4 technique than the other techniques. It was also confirmed by SIMS and I–V measurements in this study that the increasing SiH_4 flow increased the Si incorporation into Si-doped AlN layer however increased the sheet resistance because of the self-compensation effect [39,40].

Si could be incorporated up to a concentration of 7.1×10^{19} cm^{-3} for sample D1, whereas it could be incorporated up to a concentration of 1.55×10^{20} cm^{-3} for sample D3. However the AlN: Si layers were highly resistant regardless of the amount of Si incorporated. A possible explanation for the high resistance of our layers may be the formation of V_{Al}-oxygen complexes due to the high oxygen content in all epiclayers [41,42]. Also Self-compensation for high Si-concentrations reported from several groups could be a reason for high resistivity, too [43]. Silicon (Si) and oxygen (O), and their alloys are residual impurities in GaN, AlN and their alloys $Al_xGa_{1-x}N$. Studies in the literature suggested that, O plays important role in a large lattice relaxation, contributing to forming a so-called deep DX state capturing a second electron to lower its energy in AlN and $Al_xGa_{1-x}N$ with Al content above a certain level [44–47]. The process turns the shallow neutral charge state d^0 to a deep negative charge state ($2\ d^0 \rightarrow d^+ + DX^-$) and hence O behaves as a self-compensated center [45]. Some studies have discovered that Si also forms a DX state similar to O at high Al contents in AlN and $Al_xGa_{1-x}N$ [45,46]. When we examine the results of different Si doped techniques in the literature, the Si concentrations obtained in the current study have similar and better values to the results obtained with MBE (1.5×10^{20} cm^{-3}), PSD (1×10^{19} cm^{-3}) and, ion-implantation (4×10^{19} cm^{-3}) [21,48,49]. Especially, it is believed that improved contact properties in the future might help for better understanding of the electrical properties of proof of concept Si–AlN epitaxial layers.

4. Conclusion

As a result, AlN epilayers were grown on Al_2O_3 substrate using different SiH_4 flow states with MOVPE. In case of a continuous flow of SiH_4, it was observed that with the increase of SiH_4 flow rate, a higher tilt and twist formation in the sub-crystalline grains and an increase in stacking faults occurred. However, with the co-pulsed of SiH_4 and NH_3 it was thought that passivation decoration of the TDs by either the Si atoms or Si_xN_y masking. Finally, with pulsed independently SiH_4 flow condition, lower dislocation density and surface roughness were obtained.

Authors statement

I can confirm that the manuscript has been revised and approved by all named authors and that there are no other persons who satisfied the criteria for authorship but are not listed. I further confirm that the order of authors listed in the manuscript has been approved by all of us and all the authors have contribution to complete this manuscript.

Declaration of competing interest

The authors declare that they have no known competing financial interests or personal relationships that could have appeared to influence

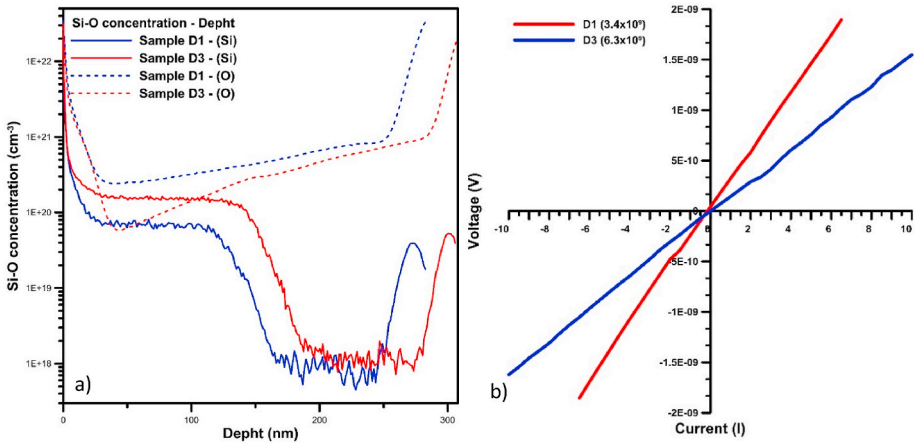

Fig. 9. a) Si and O SIMS depth profiles b) I–V measurement at 300 K.

the work reported in this paper.

Acknowledgements

The authors acknowledge the usage of the Nanophotonics Research and Application Center at Sivas Cumhuriyet University (CUNAM) facilities. This work is supported by the TUBITAK-The Scientific and Technological Research Council of Turkey, under project numbers 117F339 and 118F425.

References

[1] R. Rounds, B. Sarkar, A. Klump, C. Hartmann, T. Nagashima, R. Kirste, A. Franke, M. Bickermann, Y. Kumagai, Z. Sitar, Thermal conductivity of single-crystalline AlN, APEX 11 (2018), 071001.
[2] J. Tsao, S. Chowdhury, M. Hollis, D. Jena, N. Johnson, K. Jones, R. Kaplar, S. Rajan, C. Van de Walle, E. Bellotti, Ultrawide-bandgap semiconductors: research opportunities and challenges, Advanced Electronic Materials 4 (2018) 1600501.
[3] M. Imura, H. Sugimura, N. Okada, M. Iwaya, S. Kamiyama, H. Amano, I. Akasaki, A. Bandoh, Impact of high-temperature growth by metal-organic vapor phase epitaxy on microstructure of AlN on 6H-SiC substrates, J. Cryst. Growth 310 (2008) 2308–2313.
[4] S. Tanaka, Y. Honda, N. Sawaki, M. Hibino, Structural characterization of GaN laterally overgrown on a (111) Si substrate, Appl. Phys. Lett. 79 (2001) 955–957.
[5] S. Thapa, J. Hertkorn, F. Scholz, G. Prinz, R. Leute, M. Feneberg, K. Thonke, R. Sauer, O. Klein, J. Biskupek, Growth and studies of Si-doped AlN layers, J. Cryst. Growth 310 (2008) 4939–4941.
[6] R. Dahal, T. Al Tahtamouni, Z. Fan, J. Lin, H. Jiang, Hybrid AlN–SiC deep ultraviolet Schottky barrier photodetectors, Appl. Phys. Lett. 90 (2007) 263505.
[7] M. Hermann, F. Furtmayr, F. Morales, O. Ambacher, M. Stutzmann, M. Eickhoff, Impact of silicon incorporation on the formation of structural defects in AlN, J. Appl. Phys. 100 (2006) 113531.
[8] R. Collazo, S. Mita, J. Xie, A. Rice, J. Tweedie, R. Dalmau, Z. Sitar, Progress on n-type doping of AlGaN alloys on AlN single crystal substrates for UV optoelectronic applications, Phys. Status Solidi C 8 (2011) 2031–2033.
[9] A. Kakanakova-Georgieva, D. Nilsson, M. Stattin, U. Forsberg, Å. Haglund, A. Larsson, E. Janzén, Mg-doped Al0. 85Ga0. 15N layers grown by hot-wall MOCVD with low resistivity at room temperature, Phys. Status Solidi Rapid Res. Lett. 4 (2010) 311–313.
[10] A. Walsh, J. Buckeridge, C.R.A. Catlow, A.J. Jackson, T.W. Keal, M. Miskufova, P. Sherwood, S.A. Shevlin, M.B. Watkins, S.M. Woodley, Limits to doping of wide band gap semiconductors, Chem. Mater. 25 (2013) 2924–2926.
[11] A. Kakanakova-Georgieva, D. Nilsson, X.T. Trinh, U. Forsberg, N. Son, E. Janzén, The complex impact of silicon and oxygen on the n-type conductivity of high-Al-content AlGaN, Appl. Phys. Lett. 102 (2013) 132113.
[12] T. Kuech, Metal-organic vapor phase epitaxy of compound semiconductors, Mater. Sci. Rep. 2 (1987) 1–49.
[13] S.B. Thapa, J. Hertkorn, F. Scholz, G. Prinz, M. Feneberg, M. Schirra, K. Thonke, R. Sauer, J. Biskupek, U. Kaiser, MOVPE growth of high quality AlN layers and effects of Si doping, Phys. Status Solidi C 5 (2008) 1774–1776.
[14] M. Hermann, F. Furtmayr, A. Bergmaier, G. Dollinger, M. Stutzmann, M. Eickhoff, Highly Si-doped AlN grown by plasma-assisted molecular-beam epitaxy, Appl. Phys. Lett. 86 (2005) 192108.
[15] J.R. Creighton, G.T. Wang, W.G. Breiland, M.E. Coltrin, Nature of the parasitic chemistry during AlGaInN OMVPE, J. Cryst. Growth 261 (2004) 204–213.
[16] T.Y. Wang, J.H. Liang, G.W. Fu, D.S. Wuu, Defect annihilation mechanism of AlN buffer structures with alternating high and low V/III ratios grown by MOCVD, CrystEngComm 18 (2016) 9152–9159.
[17] I. Demir, H. Li, Y. Robin, R. McClintock, S. Elagoz, M. Razeghi, Sandwich method to grow high quality AlN by MOCVD, J. Phys. Appl. Phys. 51 (2018), 085104.
[18] I. Altuntas, M.N. Kocak, G. Yolcu, H.F. Budak, A.E. Kasapoğlu, S. Horoz, E. Gür, I. Demir, Influence of the PALE growth temperature on quality of MOVPE grown AlN/Si (111), Mater. Sci. Semicond. Process. 127 (2021) 105733.
[19] E. Calleja, M. Sánchez-Garcıa, F. Calle, F. Naranjo, E. Munoz, U. Jahn, K. Ploog, J. Sanchez, J. Calleja, K. Saarinen, Molecular beam epitaxy growth and doping of III-nitrides on Si (1 1 1): layer morphology and doping efficiency, Mater. Sci. Eng., B 82 (2001) 2–8.
[20] J.-J. Dai, C.-W. Liu, S.-K. Wu, S.-H. Huynh, J.-G. Jiang, S.-A. Yen, T.T. Mai, H.-C. Wen, W.-C. Chou, C.-W. Hu, Improving transport properties of GaN-based HEMT on Si (111) by controlling SiH4 flow rate of the SiNx nano-mask, Coatings 11 (2021) 16.
[21] T. Ive, O. Brandt, H. Kostial, K.J. Friedland, L. Däweritz, K.H. Ploog, Controlled n-type doping of AlN: Si films grown on 6H-SiC (0001) by plasma-assisted molecular beam epitaxy, Appl. Phys. Lett. 86 (2005), 024106.
[22] O. Klein, J. Biskupek, K. Forghani, F. Scholz, U. Kaiser, TEM investigations on growth interrupted samples for the correlation of the dislocation propagation and growth mode variations in AlGaN deposited on SiNx interlayers, J. Cryst. Growth 324 (2011) 63–72.
[23] S. Shetty, J. Ghatak, S. Shivaprasad, Surface nitridation induced AlN nano-columnar growth on c-sapphire, Solid State Commun. 180 (2014) 7–10.
[24] J. Wang, F. Xu, C. He, L. Zhang, L. Lu, X. Wang, Z. Qin, B. Shen, High quality AlN epilayers grown on nitrided sapphire by metal organic chemical vapor deposition, Sci. Rep. 7 (2017) 1–7.
[25] Y. Wu, A. Hanlon, J. Kaeding, R. Sharma, P. Fini, S. Nakamura, J. Speck, Effect of nitridation on polarity, microstructure, and morphology of AlN films, Appl. Phys. Lett. 84 (2004) 912–914.
[26] I. Demir, Y. Koçak, A.E. Kasapoğlu, M. Razeghi, E. Gür, S. Elagoz, AlGaN/AlN MOVPE heteroepitaxy: pulsed co-doping SiH4 and TMIn, Semicond. Sci. Technol. 34 (2019), 075028.
[27] Y. Chen, H. Wu, E. Han, G. Yue, Z. Chen, Z. Wu, G. Wang, H. Jiang, High hole concentration in p-type AlGaN by indium-surfactant-assisted Mg-delta doping, Appl. Phys. Lett. 106 (2015) 162102.
[28] Q. Dai, X. Zhang, Z. Liang, G. Yang, Z. Wu, S. Chen, J. Zhao, C. Meng, J. Wang, Y. Cui, Effects of indium surfactant on growth and characteristics of (112¯2) plane AlGaN-based multiple quantum wells, Opt. Mater. Express 8 (2018) 24–29.
[29] P. Pramanik, S. Sen, C. Singha, A.S. Roy, A. Das, S. Sen, A. Bhattacharyya, D. Kumar, D.S. Rao, Controlling the compositional inhomogeneities in AlxGa1− xN/AlyGa1− yN MQWs grown by PA-MBE: effect on luminescence properties, J. Cryst. Growth 439 (2016) 60–65.
[30] F. Brunner, A. Mogilatenko, V. Kueller, A. Knauer, M. Weyers, Stress evolution during AlxGa1− xN/AlN growth on sapphire, J. Cryst. Growth 376 (2013) 54–58.
[31] A. Knauer, F. Brunner, T. Kolbe, V. Küller, H. Rodriguez, S. Einfeldt, M. Weyers, M. Kneissl, MOVPE Growth for UV-LEDs, Light-Emitting Diodes: Materials, Devices, and Applications for Solid State Lighting XIII, International Society for Optics and Photonics, 2009, p. 72310G.
[32] T. Akasaka, T. Nishida, Y. Taniyasu, M. Kasu, T. Makimoto, N. Kobayashi, Reduction of threading dislocations in crack-free AlGaN by using multiple thin S x Al 1− x N interlayers, Appl. Phys. Lett. 83 (2003) 4140–4142.
[33] M. Kappers, R. Datta, R. Oliver, F. Rayment, M. Vickers, C. Humphreys, Threading dislocation reduction in (0 0 01) GaN thin films using SiNx interlayers, J. Cryst. Growth 300 (2007) 70–74.
[34] S. Tanaka, M. Takeuchi, Y. Aoyagi, Anti-surfactant in III-nitride epitaxy–quantum dot formation and dislocation termination, Jpn. J. Appl. Phys. 39 (2000) L831.
[35] K. Forghani, M. Klein, F. Lipski, S. Schwaiger, J. Hertkorn, R.A. Leute, F. Scholz, M. Feneberg, B. Neuschl, K. Thonke, High quality AlGaN epilayers grown on sapphire using SiNx interlayers, J. Cryst. Growth 315 (2011) 216–219.
[36] A. Mogilatenko, A. Knauer, U. Zeimer, C. Hartmann, H. Oppermann, M. Weyers, Silicon induced defect reduction in AlN template layers for epitaxial lateral overgrowth, J. Cryst. Growth 462 (2017) 18–23.

[37] H. Trodahl, F. Martin, P. Muralt, N. Setter, Raman spectroscopy of sputtered AlN films: E 2 (high) biaxial strain dependence, Appl. Phys. Lett. 89 (2006), 061905.
[38] M.N. Abd Rahman, N.A. Talik, M.I.A. Khudus, A.F. Sulaiman, K. Allif, N.M. Zahir, A. Shuhaimi, Ammonia flux tailoring on the quality of AlN epilayers grown by pulsed atomic-layer epitaxy techniques on (0 0 0 1)-oriented sapphire substrates via MOCVD, CrystEngComm 21 (2019) 2009–2017.
[39] J.M. Wagner, F. Bechstedt, Electronic and phonon deformation potentials of GaN and AlN: ab initio calculations versus experiment, Phys. Status Solidi 234 (2002) 965–969.
[40] J.S. Harris, J.N. Baker, B.E. Gaddy, I. Bryan, Z. Bryan, K.J. Mirrielees, P. Reddy, R. Collazo, Z. Sitar, D.L. Irving, On compensation in Si-doped AlN, Appl. Phys. Lett. 112 (2018) 152101.
[41] Y. Taniyasu, M. Kasu, N. Kobayashi, Intentional control of n-type conduction for Si-doped AlN and Al X Ga 1− XN (0.42⩽ x< 1), Appl. Phys. Lett. 81 (2002) 1255–1257.
[42] M. McCluskey, N. Johnson, C.G. Van de Walle, D. Bour, M. Kneissl, W. Walukiewicz, Metastability of oxygen donors in AlGaN, Phys. Rev. Lett. 80 (1998) 4008.
[43] K. Nam, M. Nakarmi, J. Lin, H. Jiang, Deep impurity transitions involving cation vacancies and complexes in AlGaN alloys, Appl. Phys. Lett. 86 (2005) 222108.
[44] M. Wagener, G. James, F. Omnès, Intrinsic compensation of silicon-doped AlGaN, Appl. Phys. Lett. 83 (2003) 4193–4195.
[45] C. Park, D. Chadi, Stability of deep donor and acceptor centers in GaN, AlN, and BN, Physical Review B 55 (1997) 12995.
[46] P. Bogusławski, J. Bernholc, Doping properties of C, Si, and Ge impurities in GaN and AlN, Phys. Rev. B 56 (1997) 9496.
[47] C.G. Van de Walle, DX-center formation in wurtzite and zinc-blende Al x Ga 1− x N, Phys. Rev. B 57 (1998) R2033.
[48] Y. Sakurai, K. Ueno, A. Kobayashi, J. Ohta, H. Miyake, H. Fujioka, Growth of Si-doped AlN on sapphire (0001) via pulsed sputtering, Apl. Mater. 6 (2018) 111103.
[49] H. Okumura, S. Suihkonen, J. Lemettinen, A. Uedono, Y. Zhang, D. Piedra, T. Palacios, AlN metal–semiconductor field-effect transistors using Si-ion implantation, Jpn. J. Appl. Phys. 57 (2018), 04FR11.